

ACOUSTIC SNR AND SINR MODELLING FOR UNDERWATER COMMUNICATIONS

PA van Walree Norwegian Defence Research Establishment FFI, Horten, Norway
B Tomasi Norwegian Research Center NORCE, Bergen, Norway

1 INTRODUCTION

Underwater acoustic communications and networks are key enablers for underwater mobile networks, which are becoming more and more relevant for scientific data collection and subsea exploration, and for autonomous inspection of offshore infrastructures. There are large differences between the propagation of radio frequency (RF) waves in air and sound in the ocean, affecting all layers of the protocol stack. Existing RF protocols are suboptimal in the subsea domain, and modulation schemes and network protocols have to be designed specifically for the underwater acoustic case, where field experiments are costly. Algorithm development is therefore largely based on channel models, which are available in many flavours.

Sophisticated acoustic models can be applied when the environment is known in detail, but this is not always feasible or needed. This paper presents simple acoustic models for the signal-to-noise ratio (SNR) and signal-to-interference-plus-noise ratio (SINR). They are based on practical spreading laws and absorption for the propagation loss, and empirical relationships for ambient noise due to distant shipping, wind, rain, and thermal noise. Applications are shown for the physical layer, illustrating the trade-offs between the choice of frequency band, communication range, and energy consumption of an acoustic modem. Applications for networking consider multiple transmitters and packet collisions, illustrating how the SINR depends on the ranges of the desired and the interfering modems, the frequency band, and interferer source level.

2 ACOUSTIC PROPAGATION AND BACKGROUND NOISE

2.1 Source level and propagation loss

Transducers are used in underwater acoustics to convert an electrical signal into sound. The term source level (SL) is a measure of the strength of the source, and is closely related to the radiated acoustic power. In ISO standard 18405 “Underwater acoustics — Terminology”, source level is formally defined as¹

$$L_S = 10 \log_{10} \left(\frac{\overline{p^2}(r) r^2}{p_0^2 r_0^2} \right) \text{ dB} \quad (1)$$

where $\overline{p^2}(r)$ is the mean-square (averaged over time) sound pressure at a distance r from a source in free space, and $p_0 = 1 \mu\text{Pa}$ and $r_0 = 1 \text{ m}$ are the accepted reference values for pressure and distance.

The intensity I is the acoustic power transferred per unit area. In a medium of density ρ and sound speed c , the mean-square sound pressure is $\bar{p}^2 = \rho c I$. For an omnidirectional source which radiates an acoustic power P , the free-space intensity is $I(r) = P/(4\pi r^2)$. The source level can be expressed as

$$L_S = 10 \log_{10} \left(\frac{\rho c P}{4\pi p_0^2 r_0^2} \right) \text{ dB} \quad (2)$$

In sea water, with $\rho \approx 1024 \text{ kg m}^{-3}$ and $c \approx 1500 \text{ m s}^{-1}$, an acoustic power $P = 1 \text{ W}$ gives $SL \approx 171 \text{ dB re } 1 \mu\text{Pa}^2\text{m}^2$.

Propagation loss (PL) is a measure of the reduction in mean-square sound pressure between a sender and a receiver. It is the difference between source level and the mean square sound pressure level (SPL) due to the signal. Denoting this SPL as the signal level $SL = 10 \log_{10}(\bar{p}^2/p_0^2)$, the PL becomes

$$PL = L_S - SL \quad (3)$$

Power and intensity are frequently used as informal synonyms of mean-square sound pressure. The distinction is unimportant for PL computations, so long as sender and receiver are located in the same medium. The dominant contributions to PL in an ocean environment are absorption and spreading loss.

2.2 Absorption

Absorption is attenuation of acoustic waves in the body of ocean water due to chemical relaxation effects and viscous damping. It is customary to specify an absorption coefficient a in decibels per unit of distance. Empirical absorption formulas have been derived, for instance by Thorp² and Francois and Garrison³. Thorp's equation is based on measurements collected in a deep ocean sound channel, and is attractive in that $a = a(f)$ only depends on the frequency. The formula of Francois and Garrison is more accurate for other environments, but requires more input parameters: $a = a(f, T, d, S, pH)$. Figure 1 compares the models, for a given environment for Francois and Garrison. Differences are noticeable, but there is consensus that absorption increases rapidly with frequency. This is a fundamental property of subsea acoustic propagation, which strongly influences design frequency bands and achievable ranges.

2.3 Shallow water and geometrical spreading laws

Modern transducers are typically omnidirectional in azimuth and fairly omnidirectional in the vertical plane. Sound is radiated in all directions, but in shallow water it becomes trapped in a waveguide whose depth and sediment type affect the PL through boundary interactions. PL can be accurately computed if detailed information on the environment is available, but a high accuracy is not always needed. For some applications, a simple geometrical spreading law of the form

$$PL = A + B \log_{10} R + a(f, \dots)r \quad (4)$$

is sufficient, where $A + B \log_{10} R$ (with $R = r/r_0$) is the loss due to spreading and $a(f, \dots)r$ the loss due to absorption. The trend of the range dependence can often be captured if A and B are carefully chosen⁵.

Spreading loss is governed by the area into which the sound has spread at a distance r from the source. Figure 2 illustrates that a shallow-water environment is characterized by range regions with different spreading factors B . Close to the source, the sound experiences free-space conditions with spherical spreading. The area into which the sound has spread is $4\pi r^2$, and the acoustic intensity is $I(r) = P/(4\pi r^2)$. The propagation loss follows as

$$PL = L_S - SL = 20 \log_{10} R + a(f, \dots)r. \quad (5)$$

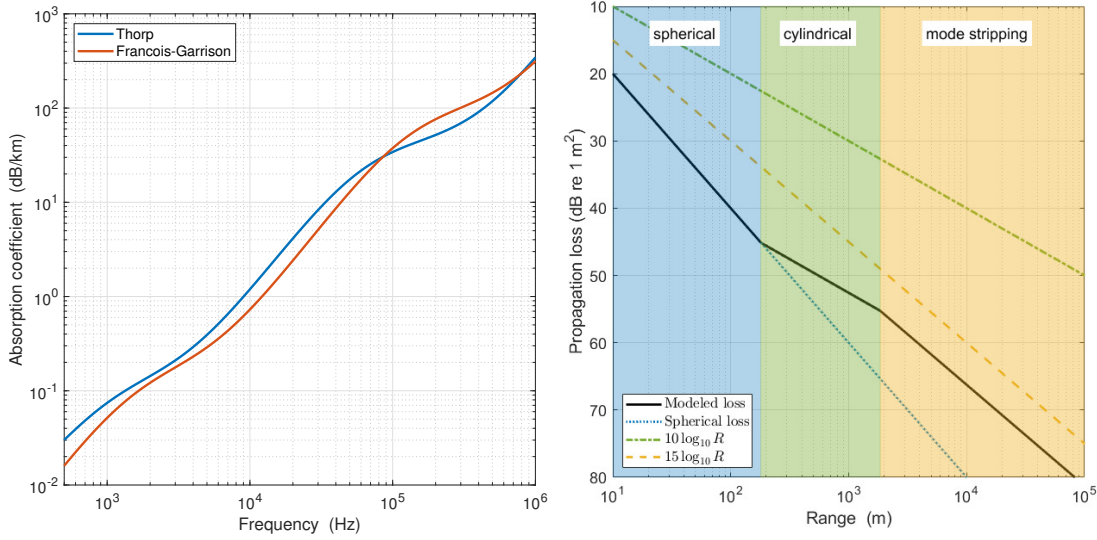


Figure 1: Left: Absorption coefficient according to Thorp² and Francois and Garrison³. The latter is computed for $T = 20^\circ\text{C}$, a depth $d = 100\text{ m}$, $S = 35\text{ g kg}^{-1}$, and $\text{pH} = 8$. Right: Propagation loss model (spreading only) for a shallow-water waveguide with $H = 200\text{ m}$ and a medium sand seafloor. The $10 \log_{10} R$ and $15 \log_{10} R$ curves are not physically meaningful, and just illustrate the error that results from setting A to zero in (4).

The character of the spreading changes when the wavefronts can no longer expand vertically. To a first approximation, paths at vertical angles steeper than a critical angle ϕ_c are refracted into the sediment, and paths below the critical angle are reflected and become trapped in the waveguide. The power remaining in the water column is $P \sin \phi_c$ and the area is $2\pi r H$. The PL becomes

$$\text{PL} = 10 \log_{10} \frac{H}{2 \sin \phi_c r_0} + 10 \log_{10} R + a(f, \dots)r. \quad (6)$$

It varies with $10 \log_{10} R$, which is known as cylindrical spreading. A more realistic seafloor model is needed for still longer ranges. The entrapment of sound is not perfect, and energy gradually dissipates after multiple bottom interactions. The effect is largest for steep paths close to ϕ_c , and can be modeled by a gradual narrowing of the angle ϕ with range. This yields the “mode-stripping” formula⁵

$$\text{PL} \approx 5 \log_{10} \left(\frac{\eta H}{\pi r_0} \right) + 15 \log_{10} R + a(f, \dots)r, \quad (7)$$

The PL varies with $15 \log_{10} R$, which is sometimes called “practical spreading”. Figure 1 shows the spreading loss for an environment with a bottom depth $H = 200\text{ m}$ and a sediment consisting of medium sand. The critical angle for medium sand is $\phi_c = 34^\circ$, and $\eta = 0.28$ ⁴.

The losses in (5), (6) and (7) agree with the generic spreading law (4). A is not independent of B , but complies with the format $A = (20 - B) \log_{10}(X/r_0)$, where X is a physical quantity with dimensions of length⁵. This term contains the losses incurred prior to entering the $B \log_{10} R$ spreading regime.

2.4 Noise and interference

Sound due to distant shipping has travelled over long distances, and is usually the dominant noise component below $\sim 500\text{ Hz}$. The frequency regime between $\sim 500\text{ Hz}$ and $\sim 50\text{ kHz}$ is dominated by wind, which

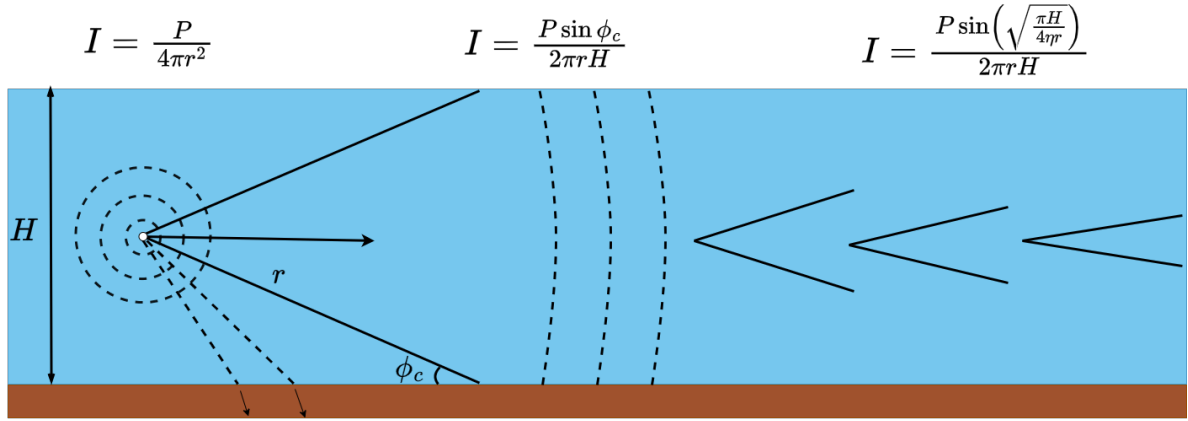


Figure 2: Illustration of a shallow-water transmission scenario with different spreading regimes.

generates noise through sea surface agitation. Rain is an intermittent but loud noise source in the same regime. Sources of acoustic noise have to be close to the receiver to be relevant at still higher frequencies, where sound is quickly attenuated by absorption. The dominant noise mechanism above ~ 50 kHz is not due to sound, but to thermal agitation of water molecules in direct contact with the receiver hydrophone.

The above sources are always present (distant shipping, wind, thermal agitation) or are likely to appear during a long-term deployment (rain). There are of course many more sources of noise and interference, like nearby ships, marine life, system self noise, and acoustic transmissions by other instruments. These sources are more incidental, usually difficult to model, and sometimes even avoidable.

Empirical equations exist for the noise spectral density of the main sources. The present paper adopts the shipping noise equation of Tollefsen and Pecknold⁶, and Ma et al.⁷ for noise due to wind and rain. Thermal noise can be expressed as an equivalent acoustic spectral density level $NSL_{th}(f) \approx -74.6 + 20 \log_{10} \left(\frac{f}{f_0} \right)$ in dB re $1 \mu Pa^2 Hz^{-1}$. Noise spectral density levels are illustrated by Fig. 3 for an example case with medium shipping in shallow water, a wind speed of $6-8 \text{ m s}^{-1}$, and light rain ($2-5 \text{ mm h}^{-1}$). The shipping noise is insignificant for the chosen frequency regime, which is dominated by wind up to 10 kHz, by rain between 10 and 100 kHz, and by thermal noise above 100 kHz. The rain-induced noise is strongest between 10 and 30 kHz, which is characteristic of the small raindrops in drizzle. Heavier rainfall contains larger drops that generate loud noise in a wider band⁷.

3 APPLICATION TO ACOUSTIC COMMUNICATIONS

3.1 Signal-to-Noise Ratio

The building blocks are in place to model the SNR of received communication signals

$$SNR = SL - NL = L_S - PL - NL, \quad (8)$$

where the noise level NL is the SPL due to the noise. The propagation loss is computed for the center frequency f_c , and the noise level in dB re $1 \mu Pa^2$ is obtained from the noise spectral density level

$$NL \approx NSL_{tot}(f_c) + 10 \log_{10}(B/f_0). \quad (9)$$

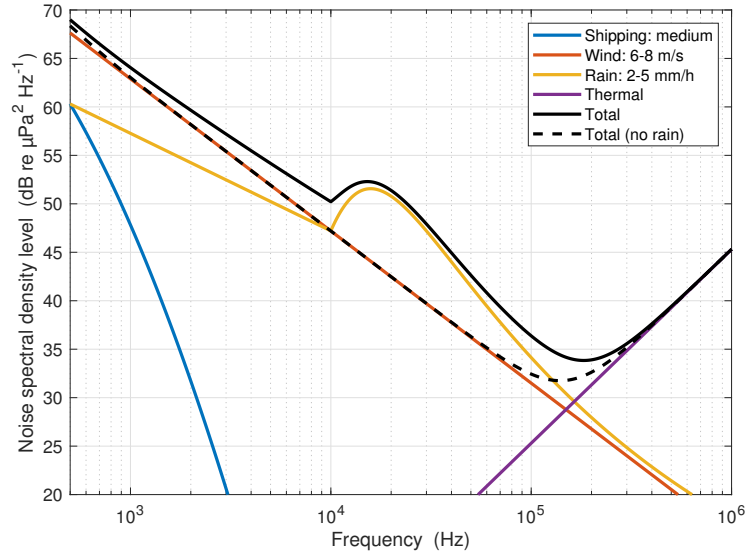


Figure 3: Noise spectral density level (NSL) due to individual sources and total level. The dash-dot curve gives the total in the absence of rain.

3.2 Scenario

The following base scenario is adopted:

- Bottom depth $H = 200$ m, medium sand sediment with $\phi_c = 34^\circ$, $\eta = 0.28^4$.
- Water: $T = 20^\circ\text{C}$, $d = 100$ m, $S = 35$ g kg $^{-1}$, pH = 8, $c = 1523$ m s $^{-1}$, $\rho = 1024$ kg m $^{-3}$.
- Ambient noise: Medium shipping in shallow water⁶, wind speed 6–8 m s $^{-1}$ and no rain.
- Modem: SL = 170 dB re 1 $\mu\text{Pa}^2\text{m}^2$, bandwidth $B = \alpha f_c = f_c/2$, spectral efficiency $\gamma = 1$ (b/s) Hz $^{-1}$.

The environment is that of Figs. 1 and 3 without rain. The sea water properties T , d , S and the pH value are input to the absorption formula of Francois and Garrison³. Acoustic communication systems are wideband, employing a bandwidth that is not small compared with the center frequency. A typical value $\alpha = 1/2$ is adopted, and f_c is varied from 500 Hz to 1 MHz. At each value of f_c , the range-dependent propagation loss (5)(6)(7) and the noise level Eq. (9) are computed. Equation (8) finally yields the SNR as a function of center frequency and range. A theoretical channel capacity based on SNR alone yields too optimistic data rates for acoustic communication systems, which are often limited by delay-Doppler spread. A practical SNR requirement of 20 dB is adopted, which provides a margin to deal with delay-Doppler spread. Excess SNR does not guarantee error-free communication in acoustic channels, but at least the system is not limited by noise for $\gamma = 1$ (b/s) Hz $^{-1}$.

3.3 Range as a function of frequency

The blue curve in the left panel of Fig. 4 shows the 20-dB SNR range for the base scenario. It is limited by the noise term in (8) at low frequencies, and by absorption at high frequencies. The other curves reveal the influence of weather and environment conditions. Each curve differs from the base scenario by only one parameter, except the green one, where both wind speed and rainfall rate are modified. Setting H to 20 m gives a shorter regime of spherical spreading, resulting in longer communication ranges at all

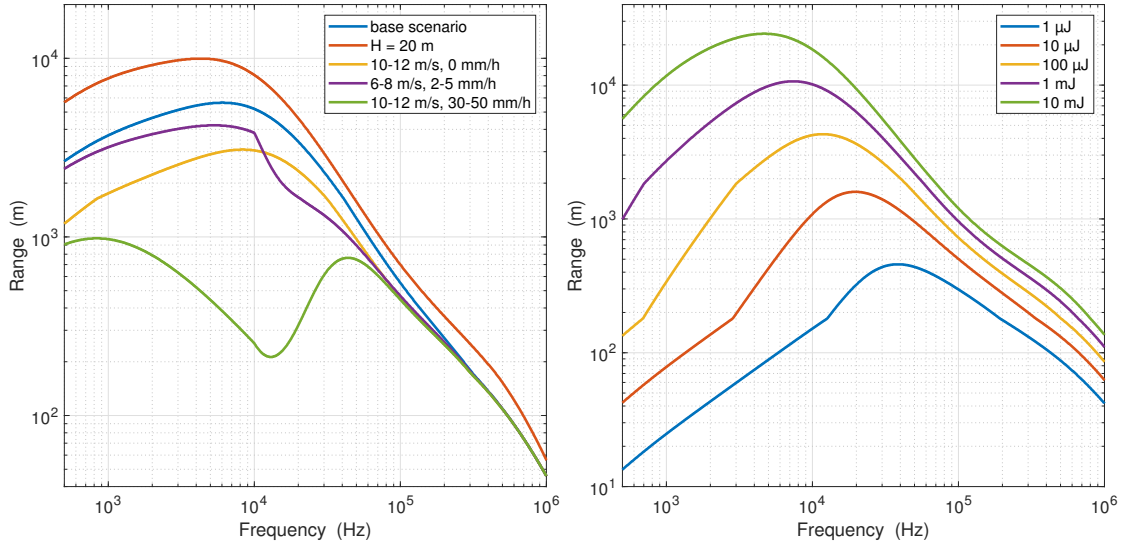


Figure 4: Left: SNR = 20 dB contours for different environment and weather conditions. Right: SNR = 20 dB contours versus the transmit energy per bit for the base scenario.

frequencies. An increase of wind speed to 10–12 m s⁻¹ reduces the range by a few km at frequencies up to a few tens of kHz. Adding light rain (2–5 mm h⁻¹) to a wind speed of 6–8 m s⁻¹ results in the noise spectral density given by the solid black curve in Fig. 3. The corresponding range reduction (purple curve in Fig. 4) is largest from 10 kHz, where the drizzle noise spectrum has a local maximum. Combining heavy rainfall with a wind speed of 10–12 m s⁻¹ (green curve) gives a drastic range reduction over a wide span of frequencies up to ~ 30 kHz. The effect is largest between 10 and 20 kHz, which is an important frequency regime for acoustic communication. Many modem vendors have models in this regime, which is also home to the JANUS standard⁸.

3.3.1 Fixed energy budget

Battery lifetime is important for subsea instrumentation, where the energy consumption of an acoustic modem can be a decisive factor. The curves in the left panel of Fig. 4 are for a given source level, which is a measure of the acoustic power. However, equal power does not imply equal energy under the constraint of a given data volume and a proportional bandwidth. The time required to transmit N information bits is $T = N/(\gamma B) = N/(\alpha \gamma f_c)$. The required energy is $E = PT = PN/(\alpha \gamma f_c)$, which decreases with frequency. If the energy is fixed instead of L_S , the power $P = \alpha \gamma f_c E/N$ becomes a function of frequency. The required source level follows from (2) as

$$L_S = 10 \log_{10} \left(\frac{\rho c \alpha \gamma E_b f_c}{4 \pi p_0^2 r_0^2} \right) \text{ dB} \quad (10)$$

where $E_b = E/N$ is the acoustic energy per bit radiated by the transmitter. The right panel of Fig. 4 illustrates the effect of E_b on the frequency-range relationship. The frequency dependence of the source level shifts the maximum range to higher frequencies as the energy budget is reduced. Long communication ranges will always require spending energy at low frequencies, but for scenarios permitting shorter link distances it pays off, energy wise, to go up in frequency. Note also that E_b is the acoustic energy per bit at the transmitter side. The electrical energy drawn from the battery is typically at least twice as high, and the common SNR metric E_b/N_0 , with N_0 the noise power spectral density, should be evaluated at the receiver side.

3.4 Collisions in acoustic networks

This section applies the propagation loss and ambient noise models to an underwater acoustic network scenario. A general network topology is assumed where transmitted signals might be simultaneously received by some of the nodes in the network. One example scenario is a multiuser single input multiple output (SIMO) star topology network where the signals from multiple transmitters have to be decoded by a single array receiver. This is a typical scenario where mobile nodes are used to communicate with a common access point. In this case, the acoustic field at each receiver element is a superposition of all the signals from N transmitters. Another example is a mesh network with a source and destination node, and intermediate relay nodes. Packet collisions may occur at any of the receiving nodes (relay or destination) with a random multiple access scheme, thus causing performance degradation.

The signal-to-interference-plus-noise metric captures the relationship between the received power of the desired signal and the power of interfering signals and noise. A simple scenario is considered where two nodes, 1 and 2, transmit to the same receiver, node 3. The acoustic field at node 3 is the superposition of the signals transmitted by nodes 1 and 2, and noise. On a linear scale, the SINR for node 1 reads

$$\text{SINR}_1 = \frac{\overline{p}_1^2(r_1)}{\overline{p}_2^2(r_2) + \overline{p}_n^2} \quad (11)$$

where $\overline{p}_1^2(r_1)$ is the received mean square pressure due to the signal of node 1, at the distance r_1 between node 1 and node 3. $\overline{p}_2^2(r_2)$ is similarly defined, and \overline{p}_n^2 is the mean square noise pressure.

Eq. (11) contains two ranges, and the propagation loss is shaped by range-dependent spreading regimes and absorption. This section investigates how the propagation loss affects the SINR as a function of frequency, source level, and the two ranges. This evaluation can be used, for example, to estimate distances at which a communication system can afford to have an interferer in the band, and therefore it has important implications for both the design of network protocols and node installations. Eq. (11) is evaluated by applying the PL model to two modem signals, before converting the computed signal and noise levels to linear space. For a given range r_1 of the intended receiver, the analysis finds the range r_2 of the interferer that yields an SINR of 20 dB. The system is limited by noise for larger values of r_2 , and by interference for smaller values. The value of 20 dB is a practical example value, just as the required SNR of 20 dB in the previous sections.

The left panel in Fig. 5 analyzes how the 20 dB contour is affected by the center frequency (and bandwidth) of the communication system. Results are shown for frequencies ranging from 1 to 100 kHz. Both nodes have a source level of 170 dB re $\mu\text{Pa}^2\text{m}^2$ and experience the ocean environment (base scenario). As expected, the acceptable interferer range decreases with the frequency. After an initial range that is limited by absorption, it is interesting to observe the different slopes of the SINR contours in different spreading regions. For example, for a system working at 25 kHz center frequency, over a range of 1 km, the interferer should be at least 4.5 km away.

The right panel in Fig. 5 analyzes the influence of the source level of the interferer. This example is for a center frequency of 10 kHz. The blue and red curves are for an interferer source level lower than that of the intended node, illustrating that the interferer can come (much) closer to the receiving node before posing problems.

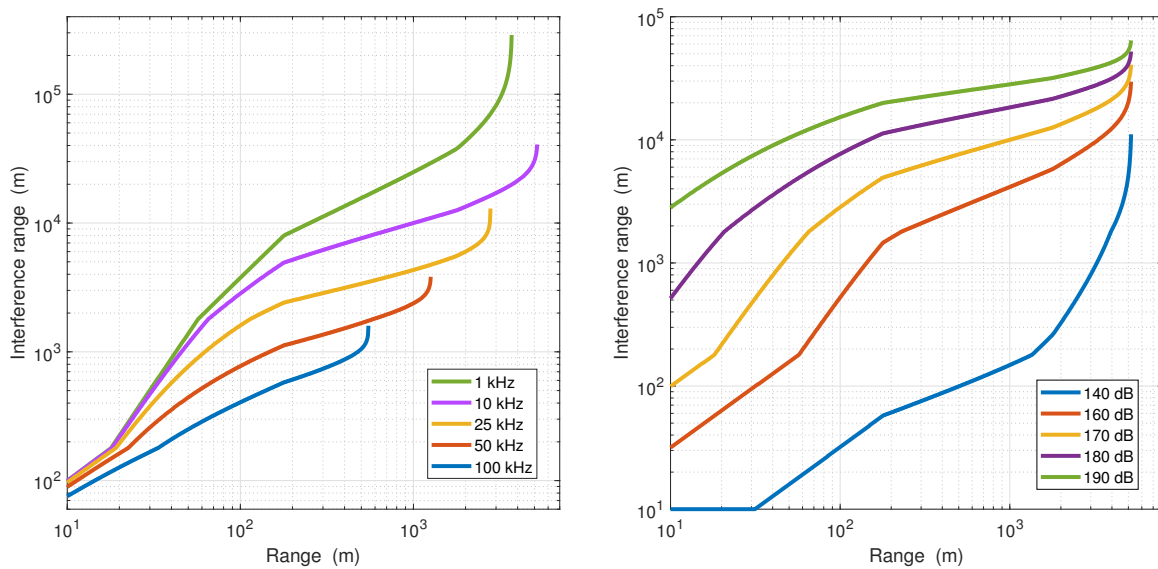


Figure 5: Left: Range relationship at different center frequencies for an interferer source level of 170 dB re $\mu\text{Pa}^2\text{m}^2$. Right: Range relationship at 10 kHz for different interferer source levels.

4 CONCLUSIONS

This paper provides guidance in selecting frequency bands and source levels for acoustic modems, given an energy budget, range requirements, and interference by other nodes in a network. The modelling uses practical spreading laws and absorption for propagation loss, and empirical relationships for ambient noise. It provides insight into acoustic propagation and how it affects design choices and trade-offs in acoustic networking, but is not a substitute for more accurate models (e.g. ray tracing) that should be used when the environment is known. Finally, it is stressed that sufficient SNR and SINR are prerequisites, but not a guarantee, for robust communication links in delay-Doppler spread channels.

REFERENCES

1. "Underwater acoustics — Terminology," ISO 18405:2017(E), International Organization for Standardization, Geneva, CH, April 2017.
2. R. J. Urick, *Principles of underwater sound*, 3rd Ed., McGraw Hill, 108 (1983).
3. R. E. Francois and G. R. Garrison, "Sound absorption based on ocean measurements. Part II: Boric acid contribution and equation for total absorption," *J. Acoust. Soc. Am.*, vol. 72, no. 6, pp. 1879–1890, December 1982.
4. M. A. Ainslie, *Principles of sonar performance modeling*, 1st ed., Springer-Verlag (2010).
5. M. A. Ainslie, P. H. Dahl, C. A. F. de Jong, and R. M. Laws, "Practical spreading laws: The snakes and ladders of shallow water acoustics," *Proc. UA2014, 2nd International Conference and Exhibition on Underwater Acoustics*, Rhodes, Greece (2014).
6. C.D.S. Tollefsen and S. Pecknold, "A simple yet practical noise model," Report DRDC-RDDC-2022-D051, Defence Research and Development Canada (2022).
7. B. B. Ma, J. A. Nystuen, and R-Ch. Lien, "Prediction of underwater sound levels from rain and wind," *J. Acoust. Soc. Am.*, vol. 117(6), 3555–3565 (2005).
8. J. Potter, J. Alves, D. Green, G. Zappa, I. Nissen, and K. McCoy, "The JANUS underwater communications standard," *Proc. IEEE UCOMMS 2014*, Sestri Levante, Italy (September 2014).